ChemBioChem

Research Article
doi.org/10.1002/cbic.202400921

Chemistry Europe
European Chemical Societies Publishing

www.chembiochem.org

# Probing Native $CB_2$ Receptor Mobility in Plasma Membranes of Living Cells by Fluorescence Recovery After Photobleaching

Francesca Ciaramellano[+],[a] Alessandro Leuti[+],[a, b] Alexandrine D. E. Kurtz,[c] Roman Sarott,[d] Matthias Westphal,[d] Patrick Pfaff,[d] Uwe Grether,[e] Erick M. Carreira,[d] Mauro Maccarrone[+],[a, f] and Sergio Oddi[+*][a, g]

In this study, we employed a novel fluorescent probe, RO7304924 – which selectively targets cannabinoid 2 receptor ($CB_2R$) – to assess the lateral mobility of $CB_2R$ within the plasma membrane of Chinese hamster ovary cells stably expressing a functional, untagged receptor variant. Utilizing confocal fluorescence recovery after photobleaching (FRAP), we quantified the diffusion coefficient and mobile fraction of $CB_2R$, thereby demonstrating the efficacy of RO7304924 as an innovative tool for elucidating the dynamics of this major endocannabinoid-binding G protein-coupled receptor. Our present findings highlight the potential of combining advanced ligand-based fluorescent probes with FRAP for future investigations into the biochemical details of $CB_2R$ mobility in living cells, and its impact on receptor-dependent cellular processes.

## 1. Introduction

The cannabinoid 2 receptor ($CB_2R$), a class A G protein-coupled receptor (GPCR), is predominantly expressed in the immune system, where it plays a critical role in modulating the initiation and resolution of inflammatory responses and immune cell activity.[1–6] Dysregulation of $CB_2R$ signalling is associated with various disorders, including autoimmune diseases, inflammatory conditions, cancer and neurodegenerative diseases.[7–13] Despite its significance, the detailed mobility characteristics of $CB_2R$ in live cells remain underexplored, with existing literature primarily focusing on $CB_2R$ pharmacology and signalling pathways.

Receptor mobility is crucial for modulating GPCR function, influencing signal transduction, receptor desensitization, and interactions with other cellular components.[14,15] Thus, elucidating $CB_2R$ dynamics within cellular membrane is relevant for understanding its biochemical function and regulation mechanisms, including those involved in various physiological and pathological states such as trafficking, internalization and recycling.[14,16,17] Techniques such as fluorescence recovery after photobleaching (FRAP) have been instrumental in studying these dynamics for various GPCRs, providing insights into their biophysical behaviour.[14,17,18] However, specific studies on $CB_2R$ using this technique are currently lacking.

To fill this gap, we performed FRAP experiments to measure the mobility of $CB_2Rs$ in living cells. We utilized a novel fluorescent probe, RO7304924, an Alexa Fluor 488-conjugated compound based on the $CB_2R$-specific agonist HU308.[19] This probe is characterized by high specificity and sensitivity for $CB_2R$ and enables rapid and precise visualization of $CB_2R$ through its receptor recognition capability (Table 1).

RO7304924 offers significant advantages over traditional labelling techniques, such as GFP-tagged receptors or antibody-based assays for studying $CB_2R$ dynamics. The key benefits of this new probe include: (*i*) preservation of native conditions, due to the non-invasive nature of RO7304924 that maintains

[a] *F. Ciaramellano,[+] A. Leuti,[+] M. Maccarrone,[+] Prof. S. Oddi[+]*
*European Center for Brain Research/Institute for Research and Health Care (IRCCS) Santa Lucia Foundation, Via del Fosso di Fiorano 64, 00143 Rome, Italy*
*E-mail: soddi@unite.it*

[b] *A. Leuti[+]*
*Department of Medicine, Campus Bio-Medico University of Rome, Rome, Italy*

[c] *A. D. E. Kurtz*
*Department of Bioscience and Technology for Food, Agriculture and Environment, University of Teramo, 64100 Teramo, Italy*

[d] *R. Sarott, M. Westphal, P. Pfaff, E. M. Carreira*
*Laboratorium für Organische Chemie, ETH Zurich, Vladimir-Prelog-Weg 3, Zurich, CH-8093, Switzerland*

[e] *U. Grether*
*Pharma Research and Early Development (pRED), Roche Innovation Center Basel, F. Hoffmann-La Roche Ltd, Grenzacherstrasse 124, Basel, CH-4070, Switzerland*

[f] *M. Maccarrone[+]*
*Department of Biotechnological and Applied Clinical Sciences, University of L'Aquila, Via Vetoio snc, 67100 L'Aquila, Italy*

[g] *Prof. S. Oddi[+]*
*Department of Veterinary Medicine, University of Teramo, via Renato Balzarini 1, 64100 Teramo, Italy*

[+] *Senior authors: Mauro Maccarrone, Prof. Sergio Oddi; Co-first authors: Francesca Ciaramellano Alessandro Leuti.*

*Supporting information for this article is available on the WWW under https://doi.org/10.1002/cbic.202400921*

**Table 1.** Main features of RO7304924 probe.

| STRUCTURE | Fluorophore | $K_i$ [nM] | | | $K_i$ ratio |
|---|---|---|---|---|---|
| | | $hCB_2R$ | $hCB_1R$ | $mCB_2R$ | ($hCB_1R$/ $hCB_2R$) |
| 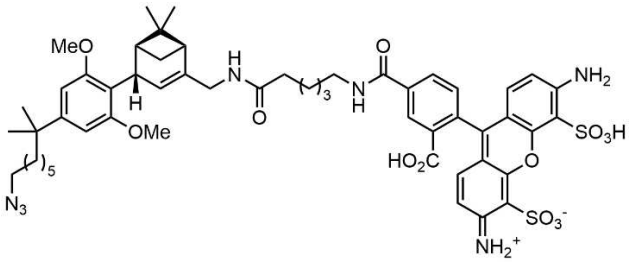 | Alexa Fluor 488 | 268 | > 10,000 | 1,204 | > 37 |

Structure and binding affinity ($K_i$) values of RO7304924 for human $CB_2R$ ($hCB_2R$), human $CB_1R$ ($hCB_1R$) and mouse $CB_2R$ ($mCB_2R$) were extracted from Ref. [19] with permission.

the native structure and biophysical properties of both the receptor and cell membranes; (*ii*) enhanced accuracy, achieved by avoiding alterations to receptor density or membrane composition, and thus enabling more refined studies of receptor dynamics; (*iii*) versatility, because the probe's design allows for application across different cell types and animal species, overcoming limitations of antibody-based techniques; and (*iv*) real-time visualization, because RO7304924 facilitates rapid and precise visualization of $CB_2R$ in living cells without the need for washing steps, enabling dynamic studies of receptor behavior. Overall, these characteristics make RO7304924 a powerful tool for investigating $CB_2R$ function in its natural cellular context, potentially leading to more physiologically relevant insights into the receptor's role in health and disease.

In this investigation, we explored the feasibility and the potential of employing FRAP with this innovative labelled chemical probe for elucidating the spatiotemporal dynamics of $CB_2Rs$ in the cellular contexts. Furthermore, we evaluated and discussed the main dynamic coefficients of $CB_2R$, such as the diffusion coefficient and the mobile fraction.

## Materials and Methods

### Reagents

Chemicals used in the experiments were of the highest analytical grade. Dulbecco's Modified Eagle Medium (DMEM), foetal bovine serum (FBS), HT supplement, and other cell culture reagents were procured from Corning (Corning, New York, NY, USA). All other chemicals were obtained from Sigma Chemical Co. (Milan, Italy), unless otherwise stated.

### Cell Culture Maintenance

Clonal cell line of Chinese hamster ovary cells, stably overexpressing the human $CB_2R$ (CHO-DUKX_HOMSA_CNR2_Clone_90_CRE-Luc), were cultivated DMEM supplemented with 10% FBS, sodium hypoxanthine (100 μM), thymidine (16 μM), penicillin (100 U/mL), and streptomycin (100 μg/mL), as previously described.[20] Culturing was carried out at 37 °C in a humidified atmosphere containing 5% $CO_2$. For selection, 200 μg/mL of hygromycin and 400 μg/mL of geneticin were added to the complete media culture.

### Time-Lapse Imaging

Cells were seeded in 8-well chamber slides (Ibidi, Gräfelfing, Germany) at a density of 100,000 cells/well and cultured for 24 hours. Subsequently, a small volume of RO7304924 (10 mM in DMSO) was mixed with 20% (w/v) Pluronic F-127 in DMSO at a ratio of 1:1 immediately before use. Before imaging, the solution of RO7304924 and Pluronic F-127 was further diluted to 0.2 μM in HEPES-buffered RPMI without phenol red and quickly added to the cells. The final concentrations are 0.008% (v/v) for DMSO and 0.002% (w/v) for Pluronic F-127. The concentration of Pluronic F-127 used in this study is consistent with concentrations employed in similar studies, as it has been demonstrated to preserve the physical and functional properties of cellular membranes at these levels (https://assets.thermofisher.com/TFS-Assets/LSG/manuals/mp03000.pdf).[21] To evaluate whether the probe needed to be removed from the culture medium before performing measurements, FRAP experiments were conducted under two conditions: with or without a washing step following probe incubation. In the washing condition, cells were incubated with the probe for 30 min and subsequently washed with fresh medium devoid of the probe prior to measurements. In the no-wash condition, the medium containing the probe was maintained throughout the FRAP measurements.

#### *Imaging Equipment*

Imaging was performed by using confocal laser scanning microscope ZEISS LSM 800, Axio Observer.Z1/7 equipped with the blue edition Zen 2.3.69.1016 software (Zeiss, Oberkochen, Germany). To maximize the resolution enhancement, a high numerical aperture oil immersion alpha Plan-Apochromat 63X/1.40 oil DIC M27 objective at 1.5 x digital was used. RO7304924 was excited using a 488 nm laser line, and the corresponding fluorescence emission was detected using a 533 nm long-pass filter. Imaging was performed using unidirectional scanning with a pinhole size set to 1 Airy Unit. Frames of 512 x 512 pixel (67.61 μm x 67.61 μm), 8 bits were acquired during the experiments.

### *FRAP Experiment Setup*

FRAP experiments were conducted at 22 ± 2 °C, following a previously published protocol.[22,23] The confocal plane was placed at the bottom cell membrane close to the glass surface and was selected for bleaching and for monitoring the recovery of fluorescence. Initially, 5 pre-bleach images (0.633 s/frame) were recorded at low laser intensity (0.6 %, 0.4 kW/cm$^2$) to assess the fluorescence intensities of the cell at the the start of the experiment (*i.e.*, the initial fluorescence). Subsequently, a circular region of interest with a 4 μm diameter was bleached using 6 scans of the full-power 488-nm laser line (power output of 10 mW, corresponding to a power density of 80 kW/cm$^2$ in the ROI). The recovery of fluorescence was then recorded by acquiring 188 images (0.663 s/frame) at 0.6 % laser intensity. Images within each experiment were collected using identical laser-power, offset, and gain setting that was adjusted to minimize the level of auto-fluorescence. Loss of fluorescence due to scanning was below 20 %.

### *Post-Imaging Processing of FRAP Data*

Fluorescence recovery was extracted from images of the bleached area and corrected for background fluorescence ($F_{BKG}$), photofading, and loss of fluorescent material due to the bleach, as well as normalized to correct for differences in protein expression levels between cells. This is achieved by normalizing the entire FRAP curve using the following equation:

$$F(t)_{norm} = \frac{F(t)_{ROI} - F_{BKG}}{F(t)_{cell} - F_{BKG}} \times \frac{F(i)_{cell} - F_{BKG}}{F(i)_{ROI} - F_{BKG}} \quad (1)$$

Where $F(t)_{ROI}$ and $F(t)_{cell}$ are the fluorescence intensities of the region of interest (ROI) and the whole cell, respectively, at each time point t. Similarly, $F(i)_{ROI}$ and $F(i)_{cell}$ represent the intensities of the ROI and the whole cell at the start of the experiment (initial time point). Finally, $F_{BKG}$ is the fluorescence intensity measured outside the cell (background fluorescence). The first part of this normalization accounts for irreversible loss of molecules owing to the bleaching event, as well as any photofading that may have occurred. To correct for this, the bleaching ROI intensity $F(t)_{ROI}$ is divided by the whole cell intensity $F(t)_{cell}$ for each time point F(t). The second part of the normalization rescales the data in terms of percentage of initial fluorescence by multiplying by the initial whole cell intensity $F(i)_{cell}$ divided by the initial intensity in the ROI, namely $F(i)_{ROI}$.

### *FRAP Data Analysis and Parameter Estimation*

Data were elaborated and analyzed statistically using R (version 4.4.0, R Foundation for Statistical Computing, Vienna, Austria; https://www.R-project.org/) within RStudio software (version 2024.04.0 + 735; https://rstudio.com/). The FRAP data were analyzed using a custom R script (Script1, available in the Supplementary Materials). To fit the fluorescence recovery curve, this script employs a nonlinear least-squares model that incorporates modified Bessel functions to account for the circular geometry of the bleached area. Nonlinear regression fitting was performed on each dataset–comprising four independent experiments derived from an average of six cells–using the following function, which describes diffusional recovery into circular regions:[24]

$$F(t)_{norm} = A \bullet e^{\frac{-2\tau}{t}} \bullet [I_0(\frac{2\tau}{t}) + I_1(\frac{2\tau}{t})] + B \quad (2)$$

where $F(t)_{norm}$ is the mean background-corrected and normalized fluorescence intensity at time t in the membrane region within the bleached region; $I_0$ and $I_1$ are modified Bessel functions of the first kind of order zero and one, respectively; B sets the fluorescence directly after the bleaching ($F_0$); and A + B determines the saturation value of the recovery ($F_\infty$). The typical diffusion time (τ) was used to calculate the diffusion coefficient (D):

$$D = \frac{r^2}{4 \bullet \tau} \quad (3)$$

where r is the radius of the circular beam (2 μm in this study).

The $M_f$ was calculated according to the following equation:

$$M_f = \frac{F_\infty - F_0}{F_i - F_0} = \frac{A}{1 - B} \quad (4)$$

where $F_\infty$ is the fluorescence in the bleached region after full recovery (A + B); $F_i$ is the fluorescence before bleaching (normalized to 1) and $F_0$ is the fluorescence just after the bleach (B). Mobile fractions are conventionally reported as a percentage; therefore, the calculated $M_f$ is multiplied by 100.

R packages used for data management and graphics included ggplot2, ggpubr, dplyr,[25] matrixStats[26] and Bessel v0.6-1.[27] The script implements a nonlinear least-squares algorithm to determine the optimal values for parameters A, B, and τ. These parameters are then used to calculate the diffusion coefficient and the $M_f$ according to the equations 2 and 3, respectively. The boxplots for $M_f$ and diffusion time (τ) were generated using another custom R script (Script 2, available in the Supplementary Materials). This script utilizes the ggplot2[25] and ggpubr[28] libraries to create detailed boxplots with individual data points overlaid. Each boxplot displays the median, quartiles, and outliers, with the mean indicated by a cross symbol. All results in the text are reported as mean ± SD.

## 2. Results and Discussion

This study aimed to characterize the dynamics of $CB_2R$ on the membrane of living cells using the confocal FRAP technique with the highly specific probe RO7304924[19] (Table 1). A suitable FRAP probe should possess several key characteristics to ensure reliable and interpretable results: (*i*) high binding affinity for the target protein (*e.g.*, human $CB_2R$) to facilitate stable interactions during imaging and recovery phases; (*ii*) high selectivity to minimize off-target effects, particularly in complex experimental systems (*e.g.*, cell lines, tissues); (*iii*) compatibility across species to allow for translational studies where relevant; (*iv*) a well-characterized mode of action (*e.g.*, agonism binding) to enable mechanistic insights; (*v*) low nonspecific binding, as excessive lipophilicity or nonspecific protein binding can obscure specific probe-receptor dynamics. (*vi*) a reporter group optimized for the intended readouts (*e.g.*, fluorescence recovery dynamics in FRAP).

Table 1 highlights the suitability of RO7304924 as a FRAP probe by demonstrating its key binding properties:

- **High affinity** for human $CB_2R$ (Ki = 268 nM), which ensures stable receptor-probe interactions during the recovery phase of FRAP experiments.

- **Exceptional selectivity** against human $CB_1R$ (Ki > 10,000 nM), with a Ki ratio > 37, underscoring its specificity and minimizing off-target interference.
- **Cross-species utility**, reflected in its moderate affinity for mouse $CB_2R$ (Ki = 1,204 nM), making the probe suitable for comparative and translational studies.

These properties are critical for achieving accurate measurements of $CB_2R$ mobility in FRAP experiments. The high affinity ensures that the probe remains associated with $CB_2R$ during the recovery phase, reducing the likelihood of dissociation events that could underestimate receptor mobility. Additionally, the probe's exceptional selectivity prevents signal contamination from $CB_1R$, thereby enhancing the reliability of the observed fluorescence recovery dynamics.

Two primary parameters were measured: mobile fraction ($M_f$), namely the proportion of receptors that are freely diffusing as opposed to being immobilized; and diffusion coefficient, which is the rate at which the receptors diffuse laterally within the membrane (Figure 1). Analysis of FRAP data revealed a remarkably high mobile fraction ($M_f$) for $CB_2R$, measured at 94 ± 3%, alongside a diffusion coefficient of 0.07 ± 0.01 $\mu m^2/s$ (Figure 1B). This elevated $M_f$ indicates that a substantial majority of $CB_2R$ molecules exhibit free diffusion within the cell membrane, suggesting minimal static binding, as well as no significant immobilization by cellular structures. In comparison, typical $M_f$ values for GPCRs assessed via FRAP assays range from 50% to 90%, depending on receptor type and specific assay conditions.[29] Notably, the observed $M_f$ for $CB_2R$ is significantly higher than that of the GFP-tagged luteinizing hormone receptor (43%) and the GFP-tagged gonadotropin-releasing hormone receptor (75%), while closely resembling that of the β-adrenergic receptor (90%).[29]

The diffusion coefficient for $CB_2R$ aligns well with values reported for other GPCRs. For instance, the GFP-tagged luteinizing hormone receptor exhibits a diffusion coefficient of 0.16 $\mu m^2/s$,[30] while the gonadotropin-releasing hormone receptor diffuses at 0.12 $\mu m^2/s$.[31] The μ-opioid receptor and $\beta_2$-adrenergic receptor show a range of diffusion coefficients from 0.04 to 0.12 $\mu m^2/s$.[31,32] Finally, the δ opioid receptor, another member of the opioid receptor family that shares some

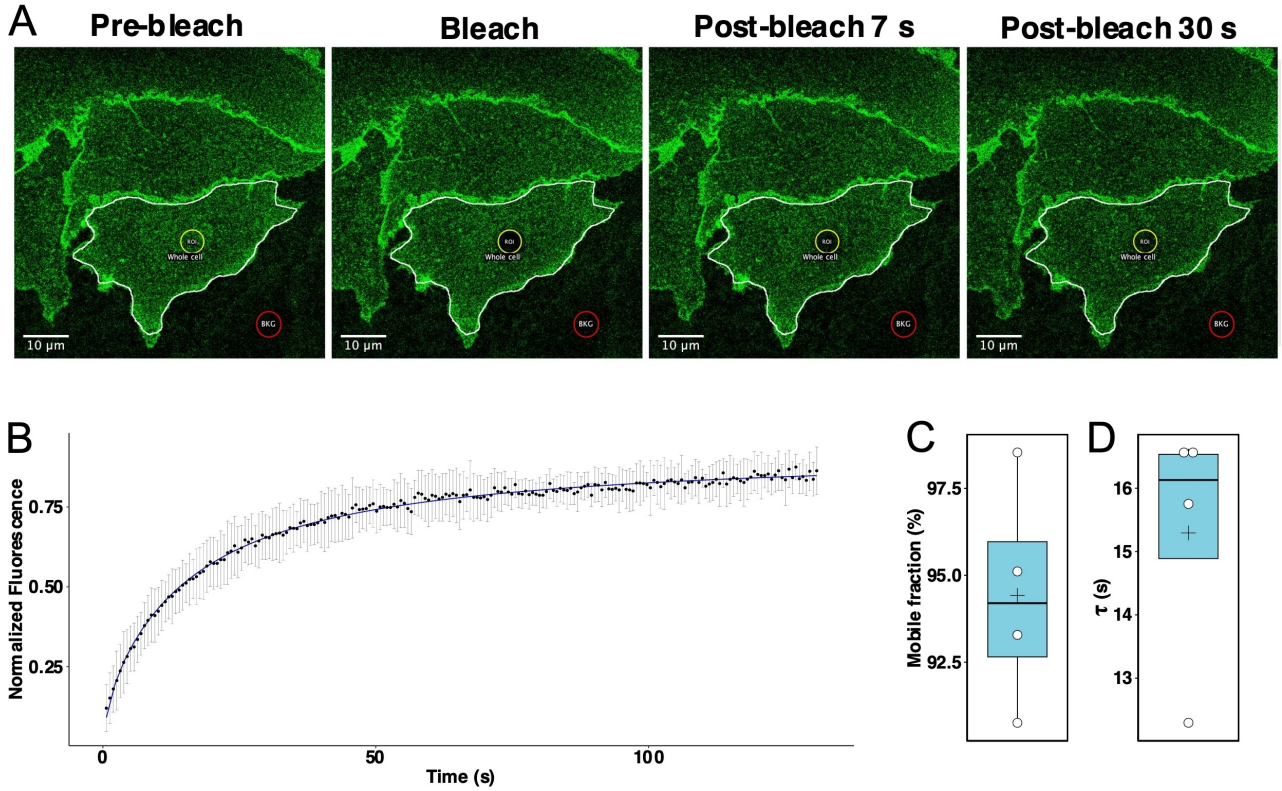


**Figure 1. Fluorescence recovery after photobleaching (FRAP) analysis.** (A) Representative confocal microscopic images depicting key stages of a FRAP experiment on CHO cells expressing human $CB_2R$ labeled with RO7304924. Images show the pre-bleach state, the bleaching event, and post-bleach recovery at 7 and 30 seconds. The confocal plane was placed at the bottom cell membrane close to the glass surface. A region of interest (ROI) of 4-μm diameter was photo-bleached, and the fluorescence recovery within this area was monitored over a time frame of 134 seconds. Simultaneously, a reference area, corresponding to the whole cell, was monitored to correct for overall bleaching, and the resulting data were normalized to the pre-bleach intensity. A third ROI, drawn on an area devoid of cells, denotes the background region (BKG). The images are representative of 4 independent experiments, and in each case, 6 cells were examined. Scale bars, 10 μm. (B) Representative FRAP recovery curve for RO7304924-labeled $CB_2R$ corrected for fluorescence decay and background fluorescence. The graph displays normalized fluorescence intensity plotted against time in seconds. Data points represent means ± SD, derived from measurements of 6 cells. The blue curve represents the mathematical fit of the FRAP data. (C) Mobile fraction (%) of plasma membrane $CB_2R$. (D) Recovery time constant (τ, in seconds) of plasma membrane $CB_2R$. For both (C) and (D), the central line in each boxplot corresponds to the median (Q2), the cross symbol (×) denotes the mean, and the box edges represent the 25th (Q1) and 75th (Q3) percentiles. Whiskers extend to the most extreme data points within 1.5 times the interquartile range from the box. The white circles overlaid on each plot represent mean values from 4 independent experiments, with each experiment analyzing 6 individual cells.

structural features with $CB_2R$, displays a diffusion coefficient of 0.085 $\mu m^2/s$.[33] These comparisons suggest that despite its high mobile fraction, $CB_2R$ demonstrates diffusion kinetics characteristic of GPCRs.

While RO7304924 does not exhibit a "fluorescent turn-on" mechanism, its fluorescence properties are strongly influenced by the microenvironment polarity and hydration. Specifically, the probe shows significantly enhanced fluorescence when bound to $CB_2R$ on the membrane. This environmentally sensitive fluorescence ensures that the signal-to-background ratio remains high, even without washing steps, as unbound probes in the aqueous phase contribute minimally to the observed fluorescence. This property represents a significant advantage for live-cell imaging and FRAP experiments, where reducing washing steps can prevent perturbations to receptor mobility or cellular integrity.

To confirm that this property does not influence the observed receptor dynamics, we performed FRAP experiments under two conditions:

1. With a washing step following probe incubation to remove unbound probes, and
2. Without washing, allowing unbound probes to remain in the aqueous phase.

The results demonstrated that both diffusion coefficient ($0.06 \pm 0.02$ $\mu m^2/s$) and $M_f$ ($98 \pm 4\%$), of $CB_2R$ remained consistent under both conditions. This finding indicates that RO7304924's high signal-to-background ratio, derived from its environmentally sensitive fluorescence, enables accurate receptor mobility measurements without requiring post-incubation washing steps.

These results suggest that the quantum yield of the RO7304924 probe is significantly modified by its binding to the receptor. While the exact mechanism remains elusive, we propose the following factors based on the literature on fluorescence modulation in protein-lipid environments: (*i*) microenvironmental polarity: the fluorescence emission maxima in methanol,[19] a moderately polar solvent, suggest that the $CB_2R$'s lipid-protein microenvironment provides an optimal polarity for fluorescence enhancement. This supports the hypothesis that fluorescence is not solely dependent on lipophilicity but also on polarity-specific stabilization of the fluorophore's excited state;[34] (*ii*) reduced solvent quenching: binding of the probe to $CB_2R$ likely shields it from the surrounding aqueous environment, thereby reducing solvent-mediated quenching effects. This interaction could explain the enhanced quantum yield observed upon receptor binding;[35] (*iii*) restricted rotational freedom: the binding pocket of $CB_2R$ may restrict the probe's rotational and vibrational degrees of freedom. Such restrictions are known to reduce non-radiative decay pathways, thereby increasing fluorescence efficiency;[36] (*iv*) structural stabilization by the receptor: The binding interaction between the probe and $CB_2R$ could stabilize the electronic and structural configuration of the fluorophore, enhancing its photophysical properties;[37] (*v*) localized concentration effect: the localization of the probe to the receptor-enriched regions of the membrane may effectively increase its apparent concentration, amplifying the fluorescence signal.[38]

## 3. Conclusions

In conclusion, in this study we provided the first characterization of $CB_2R$ mobility in plasma membranes of living cells by using FRAP and the novel fluorescent probe RO7304924 in a simplified system where $CB_2R$ is overexpressed. Even though further studies will be required in the near future to fully elucidate the behaviour of this receptor in the context of cell membranes that express physiological levels of $CB_2R$, our findings demonstrate the feasibility of using RO7304924 to study $CB_2R$ dynamics, highlighting its potential as a valuable tool for investigating receptor mobility in living systems.

## 4. Funding

This investigation was supported by the Italian Ministry of University and Research (MUR) under the competitive PRIN 2022 PNRR grant (n. P20222272N) to S.O. and M.M.

Structure and binding affinity ($K_i$) values of RO7304924 for human $CB_2R$ ($hCB_2R$), human $CB_1R$ ($hCB_1R$) and mouse $CB_2R$ ($mCB_2R$) were extracted from Ref. [19] with permission.

## *Author Contributions*

S.O. designed research. F.C. and A.L. performed the confocal microscopy and analysed the data. A.D.E.K performed cell culture. U.G., R.S., M.W., P.P. and E.M.C. contributed new reagents/analytic tools. S.O. and M.M. wrote and discussed the results.

## *Conflict of Interests*

The authors declare that they have no competing interests.

## *Data Availability Statement*

The data that support the findings of this study are available from the corresponding author upon reasonable request.

**Keywords:** membrane receptor mobility · advanced fluorescent probes · FRAP · GPCRs · cannabinoid 2 receptor

[1] A. Leuti, M. Fava, G. Forte, N. Pellegrini, S. Oddi, L. Scipioni, E. A. Gomez, J. Dalli, M. Maccarrone, *FASEB J.* **2024**, *38*, e23675.
[2] A. C. Howlett, F. Barth, T. I. Bonner, G. Cabral, P. Casellas, W. A. Devane, C. C. Felder, M. Herkenham, K. Mackie, B. R. Martin, R. Mechoulam, R. G. Pertwee, *Pharmacol. Rev.* **2002**, *54*, 161–202.
[3] K. Mackie, *J. Neuroendocrinol.* **2008**, *20*, 10–14.
[4] S. Zou, U. Kumar, *Int. J. Mol. Sci.* **2018**, *19*(3):833–855.
[5] N. Joshi, E. S. Onaivi, *Adv. Exp. Med. Biol.* **2019**, *1162*, 1–12.
[6] M. Maccarrone, V. Di Marzo, J. Gertsch, U. Grether, A. C. Howlett, T. Hua, A. Makriyannis, D. Piomelli, N. Ueda, M. van der Stelt, *Pharmacol. Rev.* **2023**, *75*, 885–958.
[7] L. Scipioni, F. Ciaramellano, V. Carnicelli, A. Leuti, A. R. Lizzi, N. De Dominicis, S. Oddi, M. Maccarrone, *Cells* **2022**, *11*(7), 1237.

[8] C. A. Lunn, E. P. Reich, L. Bober, *Expert Opin. Ther. Targets* **2006**, *10*, 653–663.
[9] S. Marino, A. I. Idris, *Pharmacol. Res.* **2017**, *119*, 391–403.
[10] L. Cristino, T. Bisogno, V. Di Marzo, *Nat. Rev. Neurol.* **2020**, *16*, 9–29.
[11] T. Bisogno, S. Oddi, A. Piccoli, D. Fazio, M. Maccarrone, *Pharmacol. Res.* **2016**, *111*, 721–730.
[12] T. Cassano, S. Calcagnini, L. Pace, F. De Marco, A. Romano, S. Gaetani, *Front. Neurol. Neurosci.* **2017**, *11*:30.
[13] Q. Xin, F. Xu, D. H. Taylor, J. Fu Zhao, J. Wu, *Acta Pharm. Sin. B* **2020**, *41*, 1507–1518.
[14] S. R. Foster, H. Bräuner-Osborne, *Handb. Exp. Pharmacol.* **2017**, *245*, 41–61.
[15] P. V. Escribá, P. B. Wedegaertner, F. M. Goñi, O. Vögler, *Biochim. Biophys. Acta Biomembr.* **2007**, *1768*, 836–852.
[16] A. J. Y. Jones, F. Gabriel, A. Tandale, D. Nietlispach, *Molecules* **2020**, *25*(20):4729.
[17] A. A. Kaczor, J. Selent, *Curr. Med. Chem.* **2011**, *18*, 4606–4634.
[18] I. Böhme, A. G. Beck-Sickinger, *Cell Commun. Signaling* **2009**, *7*, 16.
[19] R. C. Sarott, E. M. Carreira, U. Grether, M. V. Westphal, P. Pfaff, C. Korn, D. A. Sykes, T. Gazzi, B. Brennecke, K. Atz, M. Weise, Y. Mostinski, P. Hompluem, E. Koers, T. Miljuš, N. J. Roth, H. Asmelash, M. C. Vong, J. Piovesan, W. Guba, A. C. Rufer, E. A. Kusznir, S. Huber, C. Raposo, E. A. Zirwes, A. Osterwald, A. Pavlovic, S. Moes, J. Beck, I. Benito-Cuesta, T. Grande, S. R. De Martiń Esteban, A. Yeliseev, F. Drawnel, G. Widmer, D. Holzer, T. Van Der Wel, H. Mandhair, C. Y. Yuan, W. R. Drobyski, Y. Saroz, N. Grimsey, M. Honer, J. Fingerle, K. Gawrisch, J. Romero, C. J. Hillard, Z. V. Varga, M. Van Der Stelt, P. Pacher, J. Rg Gertsch, P. J. McCormick, C. Ullmer, S. Oddi, M. MacCarrone, D. B. Veprintsev, M. Nazaré, *J. Am. Chem. Soc.* **2020**, *142*, 16953–16964.
[20] T. Gazzi, B. Brennecke, K. Atz, C. Korn, D. Sykes, G. Forn-Cuni, P. Pfaff, R. C. Sarott, M. V. Westphal, Y. Mostinski, L. Mach, M. Wasinska-Kalwa, M. Weise, B. L. Hoare, T. Miljuš, M. Mexi, N. Roth, E. J. Koers, W. Guba, A. Alker, A. C. Rufer, E. A. Kusznir, S. Huber, C. Raposo, E. A. Zirwes, A. Osterwald, A. Pavlovic, S. Moes, J. Beck, M. Nettekoven, I. Benito-Cuesta, T. Grande, F. Drawnel, G. Widmer, D. Holzer, T. van der Wel, H. Mandhair, M. Honer, J. Fingerle, J. Scheffel, J. Broichhagen, K. Gawrisch, J. Romero, C. J. Hillard, Z. V. Varga, M. van der Stelt, P. Pacher, J. Gertsch, C. Ullmer, P. J. McCormick, S. Oddi, H. P. Spaink, M. Maccarrone, D. B. Veprintsev, E. M. Carreira, U. Grether, M. Nazaré, *Chem. Sci.* **2022**, *13*, 5539–5545.
[21] T. Kawanishi, L. Blank, A. Harootunian, M. Smith, R. Tsien, *J. Biol. Chem.* **1989**, *264*, 4569–4575.
[22] S. Oddi, E. Dainese, S. Sandiford, F. Fezza, M. Lanuti, V. Chiurchiù, A. Totaro, G. Catanzaro, D. Barcaroli, V. De Laurenzi, D. Centonze, S. Mukhopadhyay, J. Selent, A. C. Howlett, M. Maccarrone, *Br. J. Pharmacol.* **2012**, *165*, 2635–2651.
[23] C. A. Day, L. J. Kraft, M. Kang, A. K. Kenworthy, *Curr. Protoc. Cytom.* **2012**, *Chapter 2,* Unit2.19.
[24] D. M. Soumpasis, *Biophys. J.* **1983**, *41*, 95–97.
[25] H. Wickham, *ggplot2* **2009**, VIII, 213.
[26] H. Bengtsson, "Functions that Apply to Rows and Columns of Matrices (and to Vectors) [R package matrixStats version 1.3.0]," can be found under https://cran.r-project.org/package=matrixStats, **2024**.
[27] M. Maechler, DOI http://specfun.r-forge.r-project.org, **2022**.
[28] A. Kassambara, "'ggplot2' Based Publication Ready Plots [R package ggpubr version 0.6.0]," can be found under https://cran.r-project.org/package=ggpubr, **2023**.
[29] S. Dorsch, K. N. Klotz, S. Engelhardt, M. J. Lohse, M. Bünemann, *Nat. Methods* **2009**, *6*, 225–230.
[30] R. D. Horvat, S. Nelson, C. M. Clay, B. G. Barisas, D. A. Roess, *Biochem. Biophys. Res. Commun.* **1999**, *255*, 382–385.
[31] L. S. Barak, S. S. G. Ferguson, J. Zhang, C. Martenson, T. Meyer, M. G. Caron, *Mol. Pharmacol.* **1997**, *51*, 177–184.
[32] A. N. Saulière-Nzeh, C. Millot, M. Corbani, S. Mazères, A. Lopez, L. Salomé, *J. Biol. Chem.* **2010**, *285*, 14514–14520.
[33] J. Janáček, J. Brejchová, P. Svoboda, *Biochim. Biophys. Acta Biomembr.* **2019**, *1861*, 1346–1354.
[34] A. S. Klymchenko, *Acc. Chem. Res.* **2017**, *50*, 366–375.
[35] A. Kyrychenko, F. Wu, R. P. Thummel, J. Waluk, A. S. Ladokhin, *J. Phys. Chem. B* **2010**, *114*, 13574–13584.
[36] K. Peng, A. J. W. G. Visser, A. van Hoek, C. J. A. M. Wolfs, J. C. Sanders, M. A. Hemminga, *Eur. Biophys. J.* **1990**, *18*, 277–283.
[37] A. D. Robison, D. Huang, H. Jung, P. S. Cremer, *Biointerphases* **2013**, *8*, 1–9.
[38] B. Pradhan, S. Khatua, A. Gupta, T. Aartsma, G. Canters, M. Orrit, *J. Phys. Chem. C* **2016**, *120*, 25996–26003.

Manuscript received: November 7, 2024
Revised manuscript received: January 13, 2025
Accepted manuscript online: January 16, 2025
Version of record online: March 12, 2025